

# New Dual Conformally Invariant Off-Shell Integrals

Dung Nguyen, Marcus Spradlin and Anastasia Volovich

Brown University  
Providence, Rhode Island 02912 USA

## Abstract

Evidence has recently emerged for a hidden symmetry of scattering amplitudes in  $\mathcal{N} = 4$  super Yang-Mills theory called dual conformal symmetry. At weak coupling the presence of this symmetry has been observed through five loops, while at strong coupling the symmetry has been shown to have a natural interpretation in terms of a T-dualized  $AdS_5$ . In this paper we study dual conformally invariant off-shell four-point Feynman diagrams. We classify all such diagrams through four loops and evaluate 10 new off-shell integrals in terms of Mellin-Barnes representations, also finding explicit expressions for their infrared singularities.

## Contents

1. Introduction	1
2. Properties of Dual Conformal Integrals	3
3. Classification of Dual Conformal Diagrams	7
3.1. Algorithm	7
3.2. Results	8
4. Evaluation of Dual Conformal Integrals	10
4.1. Previously known integrals	11
4.2. New integrals	12
4.3. Infrared singularity structure	17
5. Summary	18

### 1. Introduction

Recent work on  $\mathcal{N} = 4$  super Yang-Mills theory has unlocked rich hidden structure in planar scattering amplitudes which indicates the exciting possibility of obtaining exact formulas for certain amplitudes. At weak coupling it has been observed at two and three loops [14,17] that the planar four-particle amplitude satisfies certain iterative relations which, if true to all loops, suggest that the full planar amplitude  $\mathcal{A}$  sums to the simple form

$$\log(\mathcal{A}/\mathcal{A}_{\text{tree}}) = (\text{IR divergent terms}) + \frac{f(\lambda)}{8} \log^2(t/s) + c(\lambda) + \dots, \quad (1.1)$$

where  $f(\lambda)$  is the cusp anomalous dimension,  $s$  and  $t$  are the usual Mandelstam invariants, and the dots indicate terms which vanish as the infrared regulator is removed. Evidence for similar structure in the five-particle amplitude has been found at two loops [21,22]. At strong coupling, Alday and Maldacena [27] have recently given a prescription for calculating gluon scattering amplitudes via AdS/CFT and demonstrated that the structure (1.1) holds for large  $\lambda$  as well.

An important role in this story is evidently played by a somewhat mysterious symmetry of  $\mathcal{N} = 4$  Yang-Mills theory which has been called ‘dual conformal’ symmetry in [29]. This symmetry, which is apparently unrelated to the conventional conformal symmetry of  $\mathcal{N} = 4$  Yang-Mills, acts as conformal transformations on the variables  $x_i \equiv k_i - k_{i+1}$ , where  $k_i$  are the cyclically ordered momenta of the particles participating in a scattering process. It is important to emphasize that dual conformal invariance is a property of planar amplitudes only. Although somewhat mysterious at weak coupling, the Alday-Maldacena prescription provides a geometrical interpretation which makes dual conformal symmetry

manifest at strong coupling. One of the steps in their construction involves T-dualizing along the four directions of  $AdS_5$  parallel to the boundary, and dual conformal symmetry is the just isometry of this T-dualized  $AdS_5$ .

The generalized unitarity methods [6,7,9,16,18] which are used to construct the dimensionally-regulated multiloop four-particle amplitude in  $\mathcal{N} = 4$  Yang-Mills theory express the ratio  $\mathcal{A}/\mathcal{A}_{\text{tree}}$  as a sum of certain scalar Feynman integrals—the same kinds of integrals that would appear in  $\phi^n$  theory, but with additional scalar factors in the numerator. However dimensional regularization explicitly breaks dual conformal symmetry, so the authors of [29] used an alternative regularization which consists of letting the four external momenta in these scalar integrals satisfy  $k_i^2 = \mu^2$  instead of zero. Then they observed that the particular Feynman integrals which contribute to the dimensionally-regulated amplitude are precisely those integrals which, if taken off-shell, are finite and dual conformally invariant in four dimensions (at least through five loops, which is as far as the contributing integrals are currently known [1,8,17,24,26]).

Off-shell dual conformally invariant integrals have a number of properties which make them vastly simpler to study than their on-shell cousins. First of all they are finite in four dimensions, whereas an  $L$ -loop on-shell dimensionally regulated integral has a complicated set of infrared poles starting at order  $\epsilon^{-2L}$ . Moreover in our experience it has always proven possible to obtain a one-term Mellin-Barnes representation for any off-shell integral, several examples of which are shown explicitly in section 4. In contrast, on-shell integrals typically can only be written as a sum of many (at four loops, thousands or even tens of thousands of) separate terms near  $\epsilon = 0$ . It would be inconceivable to include a full expression for any such integral in a paper.

Secondly, the relative simplicity of off-shell integrals is such that a simple analytic expression for the off-shell  $L$ -loop ladder diagram was already obtained several years ago [3,4,5] (and generalized to arbitrary dimensions in [13]). For the on-shell ladder diagram an analytic expression is well-known at one-loop, but it is again difficult to imagine that a simple analytic formula for any  $L$  might even be possible.

Finally, various off-shell integrals have been observed to satisfy apparently highly nontrivial relations called ‘magic identities’ in [23]. There it was proven that the three-loop ladder diagram and the three-loop tennis court diagram are precisely equal to each other in four dimensions when taken off-shell. Moreover a simple diagrammatic argument was given which allows one to relate various classes of integrals to each other at any number

of loops. No trace of this structure is evident when the same integrals are taken on-shell in  $4 - 2\epsilon$  dimensions.

Hopefully these last few paragraphs serve to explain our enthusiasm for off-shell integrals. Compared to our recent experience [25,31] with on-shell integrals, which required significant supercomputer time to evaluate, we find that the off-shell integrals we study here are essentially trivial to evaluate.

Unfortunately however there is a very significant drawback to working off-shell, which is that although we know (through five loops) which scalar Feynman integrals contribute to the dimensionally-regulated on-shell amplitude, we do not know which integrals contribute to the off-shell amplitude. In fact it is not even clear that one can in general provide a meaningful definition of the ‘off-shell amplitude.’ Taking  $k_i^2 = \mu^2$  in a scalar integral seems to be a relatively innocuous step but we must remember that although they are expressed in terms of scalar integrals, the amplitudes we are interested in are really those of non-abelian gauge bosons. In this light relaxing the on-shell condition  $k_i^2 = 0$  does not seem so innocent. If it is possible to consistently define a general off-shell amplitude in  $\mathcal{N} = 4$  Yang-Mills then we would expect to see as  $\mu^2 \rightarrow 0$  the universal leading infrared singularity

$$\log(\mathcal{A}/\mathcal{A}_{\text{tree}}) = -\frac{f(\lambda)}{8} \log^2(\mu^4/st) + \text{less singular terms}, \quad (1.2)$$

where  $f(\lambda)$  is the same cusp anomalous dimension appearing in (1.1). If an equation of the form (1.2) could be made to work with off-shell integrals, it would provide a method for computing the cusp anomalous dimension that is vastly simpler than that of reading it off from on-shell integrals as in [24,25,31].

The outline of this paper is as follows. In section 2 we review the definition and diagrammatic properties of dual conformal integrals. In section 3 we present the classification of off-shell dual conformal diagrams through four loops. In section 4 we evaluate 10 new dual conformal integrals in terms of Mellin-Barnes representations (finding two new ‘magic identities’) and present explicit formulas for their behaviour in the infrared limit  $\mu^2 \rightarrow 0$ .

## 2. Properties of Dual Conformal Integrals

We begin by reviewing the definition and diagrammatic properties of dual conformal integrals following [23,29]. By way of illustration we consider first the one-loop diagram shown in Fig. 1. Black lines depict the underlying scalar Feynman diagram, with each

internal line associated to a  $1/p^2$  propagator as usual. Each dotted red line indicates a numerator factor  $(p_1 + p_2 + \dots + p_n)^2$  where the  $p_i$  are the momenta flowing through the black lines that it crosses. Of course momentum conservation at each vertex guarantees that a numerator factor only depends on where the dotted red line begins and ends, not on the particular path that it traverses through the diagram.

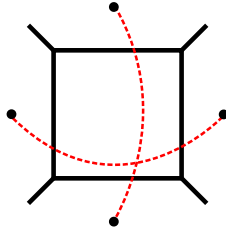


**Fig. 1:** The one-loop scalar box diagram with conformal numerator factors indicated by the dotted red lines.

We adopt a standard convention (see for example [14]) that each four-dimensional loop momentum integral comes with a normalization factor of  $1/i\pi^2$ . Thus the diagram shown in Fig. 1 corresponds to the integral

$$\mathcal{I}^{(1)}(k_1, k_2, k_3, k_4) = \int \frac{d^4 p_1}{i\pi^2} \frac{(k_1 + k_2)^2 (k_2 + k_3)^2}{p_1^2 (p_1 - k_1)^2 (p_1 - k_1 - k_2)^2 (p_1 + k_4)^2}. \quad (2.1)$$

We regulate this infrared divergent integral by taking the external legs off-shell, choosing for simplicity all of the ‘masses’  $k_i^2 = \mu^2$  to be the same. A different possible infrared regulator that one might consider would be to replace the  $1/p^2$  propagators by massive propagators  $1/(p^2 - m^2)$ , but we keep all internal lines strictly massless.

Following [23,29] we then pass to dual coordinates  $x_i$  by taking

$$k_1 = x_{12}, \quad k_2 = x_{23}, \quad k_3 = x_{34}, \quad k_4 = x_{41}, \quad p_1 = x_{15}, \quad (2.2)$$

where  $x_{ij} \equiv x_i - x_j$ , so that (2.1) becomes

$$\mathcal{I}^{(1)}(x_1, x_2, x_3, x_4) = \int \frac{d^4 x_5}{i\pi^2} \frac{x_{13}^2 x_{24}^2}{x_{15}^2 x_{25}^2 x_{35}^2 x_{45}^2}. \quad (2.3)$$

This expression is now easily seen to be invariant under arbitrary conformal transformations on the  $x_i$ . This invariance is referred to as ‘dual conformal’ symmetry in [23] because it should not be confused with the familiar conformal symmetry of  $\mathcal{N} = 4$  Yang-Mills. The

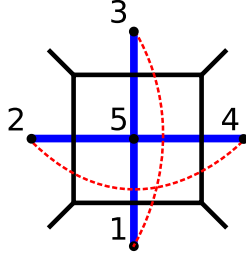


**Fig. 2:** The one-loop scalar box with dotted red lines indicating numerator factors and thick blue lines showing the dual diagram.

coordinates  $x_i$  here are momentum variables and are not simply related to the position space variables on which the usual conformal symmetry acts.

To analyze the dual conformal invariance of a diagram it is convenient to consider its dual diagram<sup>1</sup>. In Fig. 2 we have labelled the vertices of the dual diagram to Fig. 1 in accord with the expression (2.3). The numerator factors correspond to dotted red lines as before, while denominator factors in the dual expression (2.3) correspond to the thick blue lines in the dual diagram. Neighboring external faces are not connected by thick blue lines because the associated propagator is absent.

With this notation set up it is easy to formulate a diagrammatic rule for determining whether a diagram can correspond to a dual conformal integral [24]. We associate to each face in the diagram (i.e., each vertex in the dual diagram) a weight which is equal to the number of thick blue lines attached to that face minus the number of dotted red lines. Then a diagram is dual conformal if the weight of each of the four external faces is zero and the weight of each internal face is four (to cancel the weight of the corresponding loop integration  $\int d^4x$ ). Consequently, no tadpoles, bubbles or triangles are allowed in the Feynman diagram, each square must be associated with no numerator factors, each pentagon must be associated with one numerator factor, etc.

We distinguish slightly between dual conformal *diagrams* and dual conformal *integrals*. The latter are all diagrams satisfying the diagrammatic rule given above. However in [29] it was pointed out that not all dual conformal diagrams give rise to integrals that are finite off-shell in four dimensions. Those that are not finite can only be defined with a regulator

---

<sup>1</sup> The fact that nonplanar graphs do not have duals is consistent with the observation that dual conformal symmetry is apparently a property only of the planar limit.

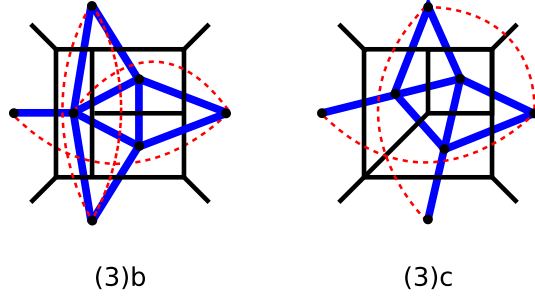


**Fig. 3:** Two examples of three-loop dual conformal diagrams.

(such as dimensional regularization) that breaks the dual conformal symmetry and hence cannot be considered dual conformal integrals.

In Fig. 3 we show two diagrams that are easily seen to be dual conformal according to the above rules. The diagram on the left is the well-known three-loop tennis court  $\mathcal{I}^{(3)b}$  [17]. The diagram on the right demonstrates a new feature that is possible only when the external lines are taken off-shell. The dotted red line connecting the top external face to the external face on the right crosses only one external line and is therefore associated with a numerator factor of  $k_i^2 = \mu^2$ . Such an integral is absent when we work on-shell. Of course *absent* does not necessarily mean that an integral *vanishes* if we first calculate it for finite  $\mu^2$  and then take  $\mu^2 \rightarrow 0$ . Indeed we will see below that  $\mathcal{I}^{(3)c} \sim \ln^3(\mu^2)$  in the infrared limit.

An important and well-known feature of four-point dual conformal integrals is that they are constrained by the symmetry to be a function only of the conformally invariant cross-ratios

$$u = \frac{x_{12}^2 x_{34}^2}{x_{13}^2 x_{24}^2}, \quad v = \frac{x_{14}^2 x_{23}^2}{x_{13}^2 x_{24}^2}. \quad (2.4)$$

Since we have chosen to take all external momenta to have the same value of  $k_i^2 = \mu^2$ , we see that  $u$  and  $v$  are actually both equal to

$$x \equiv \frac{\mu^4}{st}, \quad (2.5)$$

where  $s = (p_1 + p_2)^2$  and  $t = (p_2 + p_3)^2$  are the usual Mandelstam invariants. Therefore we can express any dual conformal integral as a function of the single variable  $x$ . One immediate consequence of this observation is that any dual conformal integral is invariant under rotations and reflections of the corresponding diagram, since  $x$  itself is invariant under such permutations. A second consequence is that any degenerate integral (by which we mean one where two or more of the external momenta enter the diagram at the same vertex) must evaluate to a constant, independent of  $x$ .

### 3. Classification of Dual Conformal Diagrams

#### 3.1. Algorithm

Let us now explain a systematic algorithm to enumerate all possible off-shell dual conformal diagrams. We use the graph generating program qgraf [2] to generate all scalar  $1\text{PI}^2$  four-point topologies with no tadpoles or bubbles, and throw away any that are non-planar or contain triangles since these cannot be made dual conformal. After these cuts there remain  $(1, 1, 4, 25)$  distinct topologies at  $(1, 2, 3, 4)$  loops respectively respectively. We adopt the naming conventions from reference [24] which displays 24 out of the 25 four-loop topologies, omitting the one we call  $h$  in Fig. 9 since it vanishes on-shell in dimensional regularization. Note also that the topologies  $e_5$  and  $c_1$  shown there are actually the same.

The next step is to try adding numerator factors to render each diagram dual conformal. Through three loops this is possible in a unique way for each topology, but at four loops there are three topologies (shown in Fig. 4) that cannot be made dual conformal at all while six topologies ( $b_1, c, d, e, e_2$  and  $f$ , shown below) each admit two distinct choices of numerator factors making the diagram dual conformal.

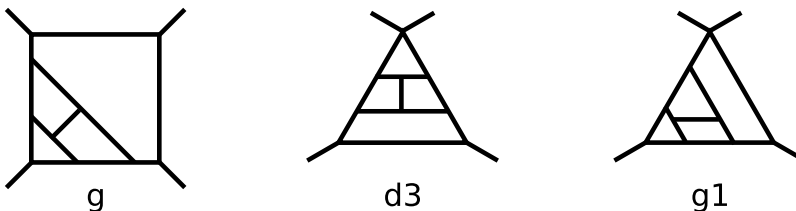


**Fig. 4:** These are the three planar four-point 1PI four-loop tadpole-, bubble- and triangle-free topologies that cannot be made into dual conformal diagrams by the addition of any numerator factors. In each case the obstruction is that there is a single pentagon whose excess weight cannot be cancelled by any numerator factor because the pentagon borders on all of the external faces. (There are no examples of this below four loops.)

We remark that we exclude from our classification certain ‘trivial’ diagrams that can be related to others by rearranging numerator factors connected only to external faces. For example, consider the two diagrams shown in Fig. 5. Clearly both are dual conformal, but they differ from each other only by an overall factor of  $x = \mu^4/st$ . In cases such as this we include in our classification only the diagram with the fewest number of  $\mu^2$  powers in the

---

<sup>2</sup> We do not know of a general proof that no one-particle reducible diagram can be dual conformal but it is easy to check through four loops that there are no such examples.



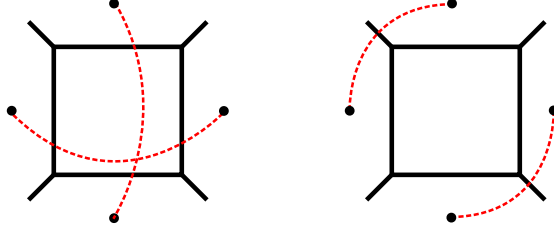


**Fig. 5:** Two dual conformal diagrams that differ only by an overall factor. As explained in the text we resolve such ambiguities by choosing the integral that is most singular in the  $\mu^2 \rightarrow 0$  limit, in this example eliminating the diagram on the right.

numerator, thereby choosing the integral that is most singular in the  $\mu^2 \rightarrow 0$  limit. In the example of Fig. 5 we therefore exclude the diagram on the right, which actually vanishes in the  $\mu^2 \rightarrow 0$  limit, in favor of the diagram on the left, which behaves like  $\ln^2(\mu^2)$ .

Another possible algorithm, which we have used to double check our results, is to first use the results of [12] to generate all planar 1PI vacuum graphs and then enumerate all possible ways of attaching four external legs so that no triangles or bubbles remain.

### 3.2. Results

Applying the algorithm just described, we find a total of  $(1, 1, 4, 28)$  distinct dual conformal diagrams respectively at  $(1, 2, 3, 4)$  loops. While  $(1, 1, 2, 10)$  of these diagrams have appeared previously in the literature on dual conformal integrals [23,24,26], the remaining  $(0, 0, 2, 18)$  that only exist off-shell are new to this paper. We classify all of these diagrams into four groups, according to whether or not they are finite in four dimensions, and according to whether or not the numerator contains any explicit factors of  $\mu^2$ . Hence we define:

Type I diagrams are finite in four dimensions and have no  $\mu^2$  factors.

Type II diagrams are divergent in four dimensions and have no  $\mu^2$  factors.

Type III diagrams are finite in four dimensions and have  $\mu^2$  factors.

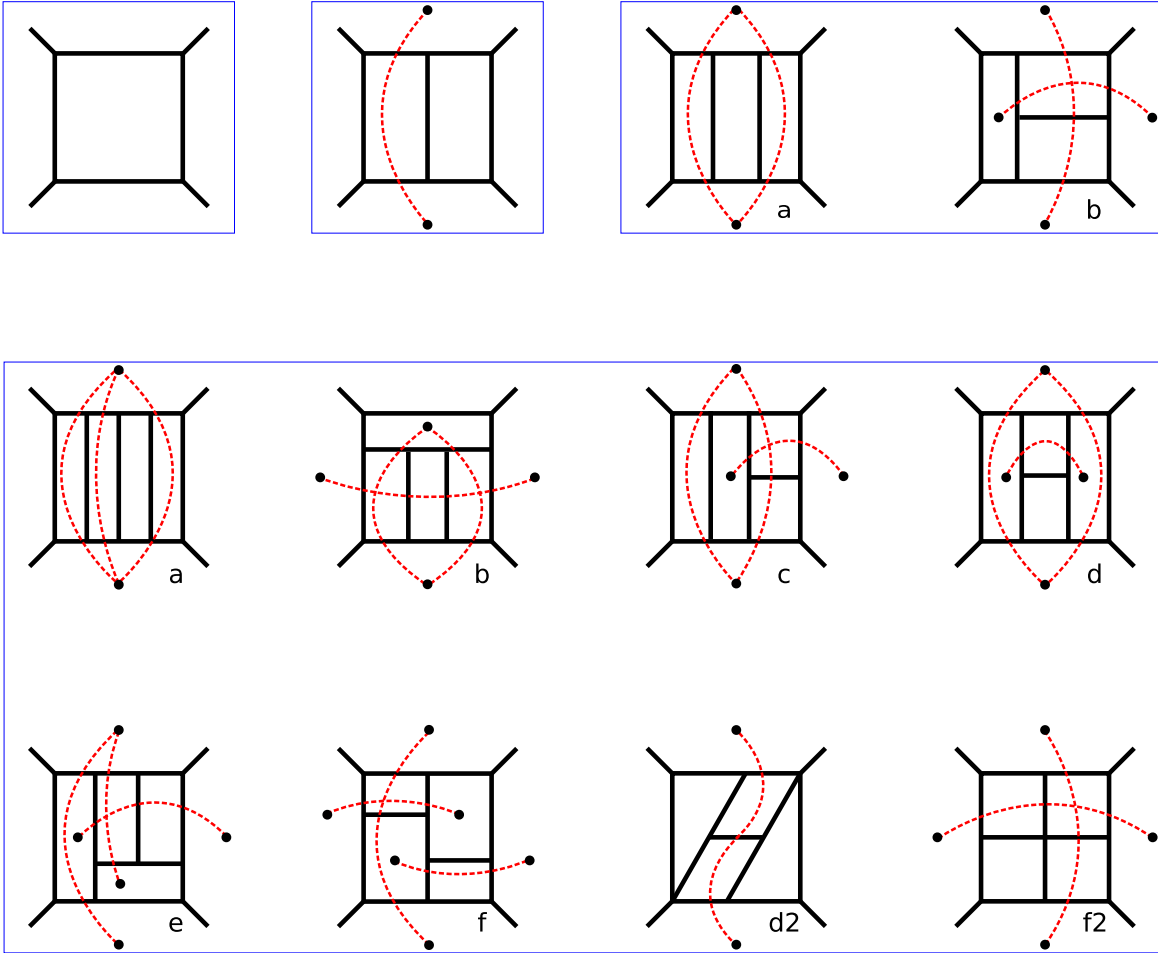
Type IV diagrams are divergent in four dimensions and have  $\mu^2$  factors.

Type I and II diagrams through five loops have been classified, and some of their properties studied, in [23,24,26,29]. In particular, it has been observed in these references that it is precisely the type I integrals that contribute to the dimensionally regulated on-shell four-particle amplitude (at least through five loops). We display these diagrams through four loops in Figs. 6 and 7. The new type III and IV diagrams that only exist off-shell are shown respectively in Figs. 8 and 9. Each diagram is given a name of the

form  $\mathcal{I}^{(L)i}$  where  $L$  denotes the number of loops and  $i$  is a label. The one- and two-loop diagrams are unique and do not require a label. Below we will also use  $\mathcal{I}^{(L)}$  to refer to the  $L$ -loop ladder diagram (specifically,  $\mathcal{I}^{(1)}$ ,  $\mathcal{I}^{(2)}$ ,  $\mathcal{I}^{(3)a}$  and  $\mathcal{I}^{(4)a}$  for  $L = 1, 2, 3, 4$ ).

We summarize the results of our classification in the following table showing the number of dual conformal diagrams of each type at each loop order:

$L$	I	II	III	IV
1	1	0	0	0
2	1	0	0	0
3	2	0	2	0
4	8	2	9	9

(3.1)


**Fig. 6:** Type I: Here we show all dual conformal diagrams through four loops that are finite off-shell in four dimensions and have no explicit numerator factors of  $\mu^2$ . These are precisely the integrals which contribute to the dimensionally-regulated on-shell four-particle amplitude [1,8,17,24]. For clarity we suppress an overall factor of  $st$  in each diagram.

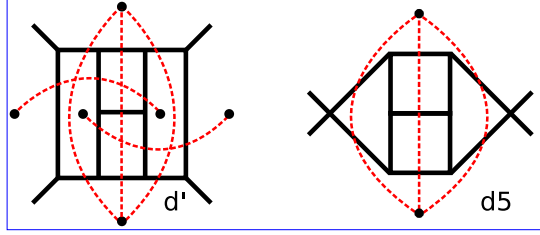


**Fig. 7:** Type II: These two diagrams have no explicit factors of  $\mu^2$  in the numerator and satisfy the diagrammatic criteria of dual conformality, but the corresponding off-shell integrals diverge in four dimensions [29]. (There are no examples of this type below four loops).

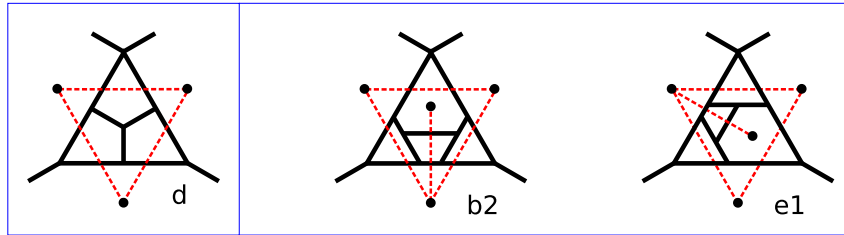
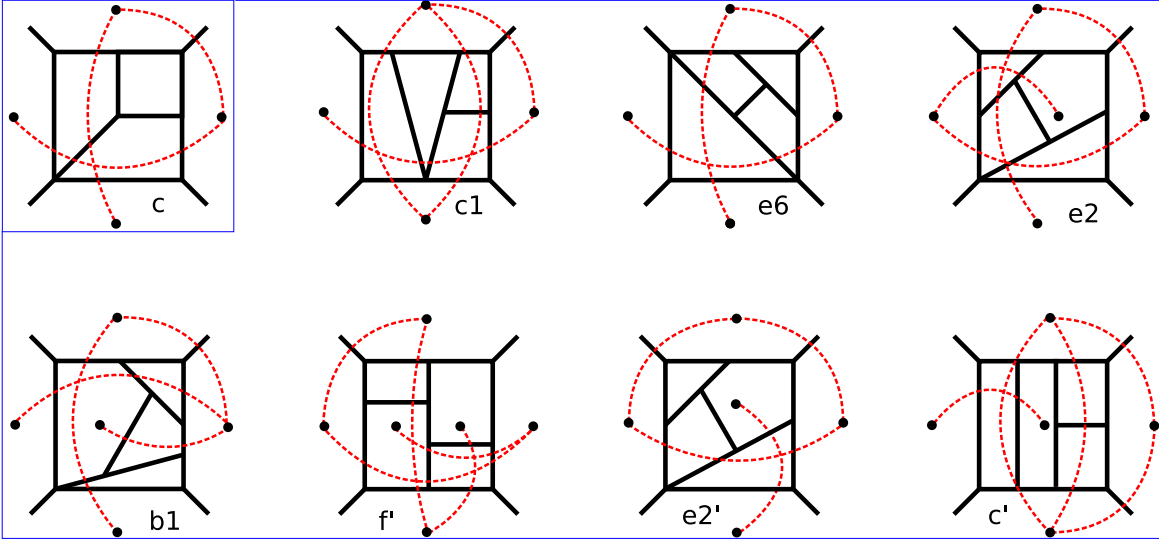


**Fig. 8:** Type III: Here we show all diagrams through four loops that correspond to dual conformal integrals in four dimensions with explicit numerator factors of  $\mu^2$ . (There are no examples of this type below three loops). In the bottom row we have isolated three degenerate diagrams which are constrained by dual conformal invariance to be equal to pure numbers (independent of  $s$ ,  $t$  and  $\mu^2$ ).

#### 4. Evaluation of Dual Conformal Integrals

In this section we describe the evaluation of dual conformal integrals. Even though

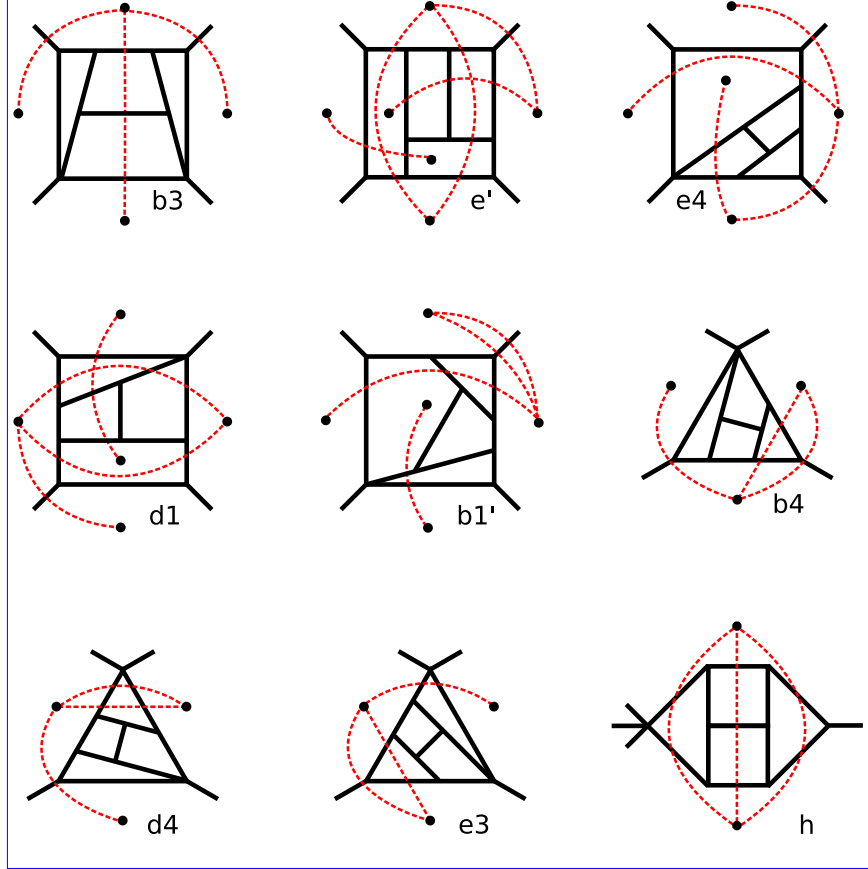


**Fig. 9:** Type IV: All remaining dual conformal diagrams. All of the corresponding off-shell integrals diverge in four dimensions.

dual conformal integrals are finite in four dimensions we evaluate them by first dimensionally regulating the integral to  $D = 4 - 2\epsilon$  dimensions, and then analytically continuing  $\epsilon$  to zero using for example algorithms described in [10,11,19]. For a true dual conformal invariant integral the result of this analytic continuation will be an integral that is finite in four dimensions, so that we can then freely set  $\epsilon = 0$ . However the type II and type IV diagrams shown in Figs. 6 and 8 turn out to not be finite in four dimensions (as can be verified either by direct calculation, or by applying the argument used in [29] to identify divergences). This leaves (1,1,4,17) integrals to be evaluated at (1,2,3,4) loops respectively.

#### 4.1. Previously known integrals

Here we briefly review the (1,1,2,5) off-shell dual conformal integrals that have already been evaluated in the literature.

The first class of integrals that have been evaluated off-shell are those corresponding to the ladder diagrams  $\mathcal{I}^{(1)}$ ,  $\mathcal{I}^{(2)}$ ,  $\mathcal{I}^{(3)a} \equiv \mathcal{I}^{(3)}$  and  $\mathcal{I}^{(4)a} \equiv \mathcal{I}^{(4)}$ . In fact an explicit formula

for the off-shell  $L$ -loop ladder diagram was given in the remarkable paper [4]. The function  $\Phi^{(L)}(x, x)$  in that paper corresponds precisely to our conventions in defining the ladder diagrams  $\mathcal{I}^{(L)}$  (including the appropriate conformal numerator factors), so we copy here their result

$$\mathcal{I}^{(L)}(x) = \frac{2}{\sqrt{1-4x}} \left[ \frac{(2L)!}{L!^2} \text{Li}_{2L}(-y) + \sum_{\substack{k,l=0 \\ k+l \text{ even}}}^L \frac{(k+l)!(1-2^{1-k-l})}{k!l!(L-k)!(L-l)!} \zeta(k+l) \log^{2L-l-k} y \right], \quad (4.1)$$

where

$$y = \frac{2x}{1-2x+\sqrt{1-4x}}. \quad (4.2)$$

The second class of integrals that have been evaluated off-shell are those that can be proven equal to  $\mathcal{I}^{(L)}$  using the ‘magic identities’ of [23]. There it was shown that

$$\mathcal{I}^{(3)a} = \mathcal{I}^{(3)b} = \mathcal{I}^{(3)} \quad (4.3)$$

and

$$\mathcal{I}^{(4)a} = \mathcal{I}^{(4)b} = \mathcal{I}^{(4)c} = \mathcal{I}^{(4)d} = \mathcal{I}^{(4)e} = \mathcal{I}^{(4)}. \quad (4.4)$$

These identities appear to be highly nontrivial and are only valid for the off-shell integrals in four dimensions; certainly no hint of any relation between these integrals is apparent when they are taken on-shell and evaluated in  $4-2\epsilon$  dimensions as in [17,24,31]. Moreover in [23] the relations (4.3) and (4.4) were given a simple diagrammatic interpretation which can be utilized to systematically identify equalities between certain integrals at any number of loops.

#### 4.2. New integrals

As indicated above we evaluate these integrals by starting with Mellin-Barnes representations in  $4-2\epsilon$  dimensions and then analytically continuing  $\epsilon$  to zero. A very useful Mathematica code which automates this process has been written by Czakon [19]. We found however that this implementation was too slow to handle some of the new integrals in a reasonable amount of time so we implemented the algorithm in a C program instead. The most difficult off-shell integral we have evaluated,  $\mathcal{I}^{(4)f^2}$ , starts off in  $4-2\epsilon$  dimensions as a 24-fold Mellin-Barnes representation (far more complicated than any of the on-shell four-loop integrals considered in [24,25], which require at most 14-fold representations), yet the analytic continuation to 4 dimensions takes only a fraction of a second in C. In what

follows we display Mellin-Barnes representations for the various integrals in 4 dimensions, after the analytic continuation has been performed and  $\epsilon$  has been set to zero.

The most surprising aspect of the formulas given below is that we are able to write each integral in terms of just a single Mellin-Barnes integral in four dimensions. This stands in stark contrast to dimensionally regulated on-shell integrals, for which the analytic continuation towards  $\epsilon = 0$  can generate (at four loops, for example) thousands or even tens of thousands of terms. For the off-shell integrals studied here something rather amazing happens: the analytic continuation still produces thousands of terms (or more), but for each off-shell integral it turns out that only one of the resulting terms is non-vanishing at  $\epsilon = 0$ , leaving in each case only a single Mellin-Barnes integral in four dimensions.

This surprising result is not automatic but depends on a number of factors, including the choice of initial Mellin-Barnes representation, the choice of integration contour for the Mellin-Barnes variables  $z_i$ , and some details of the how the analytic continuation is carried out. All of these steps involve highly non-unique choices, and by making different choices it is easy to end up with more than one term that is finite in four dimensions. However in such cases it is always possible to ‘reassemble’ the finite terms into the one-term representations shown here by shifting the contours of the remaining integration variables.

For the new 3-loop integrals, both shown in Fig. 8, we find the Mellin-Barnes representations<sup>3</sup>

$$\begin{aligned}
\mathcal{I}^{(3)c} = & - \int \frac{d^5 z}{(2\pi i)^5} x^{z_2} \Gamma(-z_1)\Gamma(-z_2)\Gamma(z_2 + 1)\Gamma(-z_2 + z_3 + 1)\Gamma(z_1 + z_3 - z_4 + 1) \\
& \Gamma(-z_4)^2\Gamma(z_4 - z_3)\Gamma(-z_2 - z_5)^2\Gamma(z_1 - z_4 - z_5 + 1) \\
& \Gamma(z_1 - z_2 + z_3 - z_4 - z_5 + 1)\Gamma(-z_1 + z_4 + z_5)\Gamma(z_2 + z_4 + z_5 + 1) \\
& \Gamma(-z_1 + z_2 + z_4 + z_5)\Gamma(-z_1 - z_3 + z_4 + z_5 - 1)/(\Gamma(1 - z_4)) \\
& \Gamma(-z_2 - z_5 + 1)\Gamma(z_1 - z_2 + z_3 - z_4 - z_5 + 2)\Gamma(-z_1 - z_2 + z_4 + z_5) \\
& \Gamma(-z_1 + z_2 + z_4 + z_5 + 1)
\end{aligned} \tag{4.5}$$

---

<sup>3</sup> All formulas in this section are valid when the integration contours for the  $z_i$  are chosen to be straight lines parallel to the imaginary axis and such that the arguments of all  $\Gamma$  functions in the numerator of the integrand have positive real part.

and

$$\begin{aligned}
\mathcal{I}^{(3)d} = & \int \frac{d^4 z}{(2\pi i)^z} \Gamma(-z_1)\Gamma(z_1+1)\Gamma(-z_2)\Gamma(z_1+z_2-z_3+1)\Gamma(-z_3)^2\Gamma(z_3-z_1) \\
& \Gamma(z_2-z_3-z_4+1)\Gamma(z_1+z_2-z_3-z_4+1)\Gamma(-z_4)^2\Gamma(z_3+z_4+1) \\
& \Gamma(-z_2+z_3+z_4)\Gamma(-z_1-z_2+z_3+z_4)/(\Gamma(1-z_1)\Gamma(1-z_3)\Gamma(1-z_4) \\
& \Gamma(z_1+z_2-z_3-z_4+2)\Gamma(-z_2+z_3+z_4+1)).
\end{aligned} \tag{4.6}$$

As expected,  $\mathcal{I}^{(3)d}$  is  $x$ -independent because the corresponding diagram is degenerate. Upon evaluating (4.6) numerically (using CUBA [15]) we find

$$\mathcal{I}^{(3)d} \approx 20.73855510 \tag{4.7}$$

with a reported estimated numerical uncertainty smaller than the last digit shown.

Finally we have 12 off-shell four-loop integrals left to evaluate, corresponding to the 9 diagrams shown in Fig. 8, along with three of the diagrams ( $\mathcal{I}^{(4)f}$ ,  $\mathcal{I}^{(4)d2}$  and  $\mathcal{I}^{(4)f2}$ ) from Fig. 6. It turns out that 4 of these 12 integrals ( $\mathcal{I}^{(4)f}$ ,  $\mathcal{I}^{(4)f'}$ ,  $\mathcal{I}^{(4)e2'}$  and  $\mathcal{I}^{(4)c'}$ ) are significantly more difficult than the rest because they apparently require analytic continuation not only in  $\epsilon$  but also in a second parameter  $\nu$  parameterizing the power of the numerator factors. (That is, the integrals initially converge only for  $\nu < 1$  and must be analytically continued to  $\nu = 1$ .) We postpone the study of these more complicated integrals to future work.

In analyzing the remaining 8 off-shell four-loop integrals we have found two new ‘magic identities’,

$$\mathcal{I}^{(4)e2} = \mathcal{I}^{(4)b1}, \quad \mathcal{I}^{(4)c1} = -\mathcal{I}^{(4)d2}. \tag{4.8}$$

We established these results directly by deriving Mellin-Barnes representations for these integrals and showing that they can be related to each other under a suitable change of integration variables. It would certainly be interesting to understand the origin of the relations (4.8) and to see whether the insight gained thereby can be used to relate various dual conformal integrals at higher loops to each other.

Mellin-Barnes representations for the 8 off-shell four-loop integrals are:

$$\begin{aligned}
\mathcal{I}^{(4)c1} = -\mathcal{I}^{(4)d2} = & - \int \frac{d^7 z}{(2\pi i)^7} x^{z_2} \Gamma(-z_1 - 1) \Gamma(z_1 + 2) \Gamma(-z_2) \Gamma(z_2 + 1) \\
& \Gamma(-z_1 - z_3 - 1) \Gamma(-z_3) \Gamma(z_3 - z_2) \Gamma(z_1 - z_2 + z_3 + 1) \Gamma(-z_4) \\
& \Gamma(z_1 - z_2 + z_3 + z_5 + 2) \Gamma(-z_6)^2 \Gamma(z_4 + z_5 - z_7 + 1) \\
& \Gamma(-z_1 + z_2 + z_4 - z_6 - z_7) \Gamma(z_4 + z_5 - z_6 - z_7 + 1) \Gamma(-z_7)^2 \Gamma(z_7 - z_5) \\
& \Gamma(z_6 + z_7 + 1) \Gamma(-z_4 + z_6 + z_7) \Gamma(-z_3 - z_4 - z_5 + z_6 + z_7 - 1) / \\
& (\Gamma(-z_1 - z_2 - 1) \Gamma(1 - z_3) \Gamma(z_1 - z_2 + z_3 + 2) \Gamma(1 - z_6) \Gamma(1 - z_7) \\
& \Gamma(z_4 + z_5 - z_6 - z_7 + 2) \Gamma(-z_4 + z_6 + z_7 + 1))
\end{aligned} \tag{4.9}$$

$$\begin{aligned}
\mathcal{I}^{(4)f2} = & \int \frac{d^{10} z}{(2\pi i)^{10}} x^{z_1} \Gamma(-z_1 - z_{10})^2 \Gamma(-z_2) \Gamma(-z_3) \Gamma(z_1 + z_{10} + z_3 + 1)^2 \Gamma(-z_4) \\
& \Gamma(-z_5) \Gamma(-z_6) \Gamma(z_{10} + z_2 + z_6) \Gamma(-z_7)^2 \Gamma(z_4 + z_7 + 1)^2 \\
& \Gamma(-z_1 - z_4 - z_5 - z_8 - 2) (-z_1 - z_{10} - z_2 - z_4 - z_6 - z_7 - z_8 - 2) \\
& \Gamma(-z_8) \Gamma(z_1 + z_8 + 2) (z_2 + z_4 + z_5 + z_7 + z_8 + 2) \\
& \Gamma(-z_2 - z_3 - z_4 - z_5 - z_9 - 2) \Gamma(-z_{10} - z_2 - z_3 - z_6 - z_9) \Gamma(-z_9) \\
& \Gamma(z_1 + z_{10} + z_2 + z_3 + z_6 + z_9 + 2) \\
& \Gamma(z_{10} + z_2 + z_3 + z_4 + z_5 + z_6 + z_9 + 2) \Gamma(-z_1 + z_3 - z_8 + z_9) \\
& \Gamma(z_2 + z_4 + z_5 + z_6 + z_8 + z_9 + 2) / (\Gamma(z_1 + z_{10} + z_3 + 2) \Gamma(-z_4 - z_5)) \\
& \Gamma(-z_1 - z_{10} - z_7) \Gamma(z_4 + z_7 + 2) \Gamma(-z_1 - z_{10} - z_2 - z_6 - z_8) \\
& \Gamma(-z_3 - z_9) \Gamma(-z_1 + z_{10} + z_2 + z_3 + z_6 - z_8 + z_9) \\
& \Gamma(z_1 + z_{10} + z_2 + z_3 + z_4 + z_5 + z_6 + z_8 + z_9 + 4)
\end{aligned} \tag{4.10}$$

$$\begin{aligned}
\mathcal{I}^{(4)e6} = & - \int \frac{d^5 z}{(2\pi i)^5} x^{z_2} \Gamma(-z_1) \Gamma(-z_2)^4 \Gamma(z_2 + 1)^2 \Gamma(-z_3) \Gamma(z_3 + 1) \\
& \Gamma(z_1 + z_3 - z_4 + 1) \Gamma(-z_4)^2 \Gamma(z_4 - z_3) \Gamma(z_1 - z_4 - z_5 + 1) \\
& \Gamma(z_1 + z_3 - z_4 - z_5 + 1) \Gamma(-z_5)^2 \Gamma(z_4 + z_5 + 1) \Gamma(-z_1 + z_4 + z_5) \\
& \Gamma(-z_1 - z_3 + z_4 + z_5) / (\Gamma(-2z_2) \Gamma(1 - z_3) \Gamma(1 - z_4) \Gamma(1 - z_5)) \\
& \Gamma(z_1 + z_3 - z_4 - z_5 + 2) \Gamma(-z_1 + z_4 + z_5 + 1)
\end{aligned} \tag{4.11}$$



$$\begin{aligned}
\mathcal{I}^{(4)e2} = \mathcal{I}^{(4)b1} = & - \int \frac{d^7 z}{(2\pi i)^7} x^{z_3} \Gamma(-z_1)\Gamma(-z_3)\Gamma(z_3+1)\Gamma(z_3-z_2)\Gamma(-z_4)^2 \\
& \Gamma(z_2-z_3+z_4+1)^2\Gamma(-z_5)^2\Gamma(z_1+z_2-z_5-z_6+2)\Gamma(-z_6)^2 \\
& \Gamma(z_5+z_6+1)\Gamma(-z_1-z_2+z_5+z_6-1)\Gamma(-z_1-z_2+z_3+z_5+z_6-1) \\
& \Gamma(-z_4+z_5-z_7)\Gamma(-z_1-z_2-z_4+z_5+z_6-z_7-1)\Gamma(-z_7) \\
& \Gamma(-z_3+z_4+z_7)\Gamma(z_1+z_2-z_3+z_4-z_5+z_7+2) \\
& \Gamma(z_1-z_5-z_6+z_7+1)/(\Gamma(z_2-z_3+z_4-z_5+2)\Gamma(-z_4-z_6+1) \\
& \Gamma(-z_1-z_2-z_3+z_5+z_6-1)\Gamma(-z_1-z_2+z_3+z_5+z_6) \\
& \Gamma(-z_4-z_7+1)\Gamma(z_1+z_2-z_3+z_4-z_5-z_6+z_7+2))
\end{aligned} \tag{4.12}$$

$$\begin{aligned}
\mathcal{I}^{(4)b2} = \mathcal{I}^{(4)e1} = & \int \frac{d^6 z}{(2\pi i)^6} \Gamma(-z_1)\Gamma(-z_2)\Gamma(-z_3)\Gamma(z_3+1)\Gamma(-z_1-z_2-z_4-2) \\
& \Gamma(-z_1-z_2-z_3-z_4-2)\Gamma(-z_4) \\
& \Gamma(z_1+z_2+z_4+3)\Gamma(z_1+z_2+z_3+z_4+3)\Gamma(z_1+z_3-z_5+1)\Gamma(-z_5) \\
& \Gamma(z_5-z_3)\Gamma(z_2+z_4+z_5+2)\Gamma(-z_4-z_5-z_6-1)\Gamma(-z_6)^2 \\
& \Gamma(z_4+z_6+1)^2\Gamma(z_2+z_4+z_5+z_6+2)/(\Gamma(1-z_3) \\
& \Gamma(-z_1-z_2-z_4-1)\Gamma(z_1+z_2+z_3+z_4+4)\Gamma(1-z_5) \\
& \Gamma(z_2+z_4+z_5+3)\Gamma(1-z_6)\Gamma(z_4+z_6+2))
\end{aligned} \tag{4.13}$$

We do not consider the equality of the two degenerate integrals  $\mathcal{I}^{(4)b2} = \mathcal{I}^{(4)e1}$  to be a ‘magic’ identity since it is easily seen to be a trivial consequence of dual conformal invariance. Evaluating them numerically we find

$$\mathcal{I}^{(4)b2} = \mathcal{I}^{(4)e1} = 70.59, \tag{4.14}$$

again with a reported estimated numerical uncertainty smaller than the last digit shown.

It would certainly be interesting to obtain fully explicit analytic results for these new integrals. Although this might seem to be a formidable challenge, the fact that it has been possible for the ladder diagrams (4.1) suggests that there is hope.

### 4.3. Infrared singularity structure

Finally, it is clearly of interest to isolate the infrared singularities of the various integrals. For the previously known integrals reviewed in subsection 3.1 we expand (4.1) for small  $x$ , finding

$$\begin{aligned}
\mathcal{I}^{(1)} &= \log^2 x + \mathcal{O}(1) \\
\mathcal{I}^{(2)} &= \frac{1}{4} \log^4 x + \frac{\pi^2}{2} \log^2 x + \mathcal{O}(1), \\
\mathcal{I}^{(3)} &= \frac{1}{36} \log^6 x + \frac{5\pi^2}{36} \log^4 x + \frac{7\pi^4}{36} \log^2 x + \mathcal{O}(1), \\
\mathcal{I}^{(4)} &= \frac{1}{576} \log^8 x + \frac{7\pi^2}{432} \log^6 x + \frac{49\pi^4}{864} \log^4 x + \frac{31\pi^6}{432} \log^2 x + \mathcal{O}(1).
\end{aligned} \tag{4.15}$$

For the new integrals evaluated in this paper we obtain the small  $x$  expansion directly from the Mellin-Barnes representations given in section 3.2 by writing each one in the form

$$\int \frac{dy}{2\pi i} x^y F(y), \tag{4.16}$$

shifting the  $y$  contour of integration to the left until it sits directly on the imaginary axis (picking up terms along the way from any poles crossed), expanding the resulting integrand around  $y = 0$  and then using the fact that the coefficient of the  $1/y^k$  singularity at  $y = 0$  corresponds in  $x$  space to the coefficient of the  $\frac{(-1)^k}{k!} \log^k x$  singularity at  $x = 0$ . In this manner we find

$$\mathcal{I}^{(3)c} = \frac{\zeta(3)}{3} \log^3 x - \frac{\pi^4}{30} \log^2 x + 14.32388625 \log x + \mathcal{O}(1) \tag{4.17}$$

at three loops and

$$\begin{aligned}
\mathcal{I}^{(4)d2} = -\mathcal{I}^{(4)e1} &= -\frac{\zeta(3)}{12} \log^5 x + \frac{7\pi^4}{720} \log^4 x - 6.75193310 \log^3 x \\
&\quad + 15.45727322 \log^2 x - 41.26913 \log x + \mathcal{O}(1), \\
\mathcal{I}^{(4)f2} &= \frac{1}{144} \log^8 x + \frac{7\pi^2}{108} \log^6 x + \frac{149\pi^4}{1080} \log^4 x \\
&\quad + 64.34694867 \log^2 x + \mathcal{O}(1), \\
\mathcal{I}^{(4)e6} &= -20.73855510 \log^2 x + \mathcal{O}(1), \\
\mathcal{I}^{(4)e2} = \mathcal{I}^{(4)b1} &= -\frac{\pi^4}{720} \log^4 x + 1.72821293 \log^3 x \\
&\quad - 12.84395616 \log^2 x + 52.34900 \log x + \mathcal{O}(1)
\end{aligned} \tag{4.18}$$

at four loops, where some coefficients have only been evaluated numerically with an estimated uncertainty smaller than the last digit shown. Interestingly, the coefficient of  $\log^2 x$  in  $\mathcal{I}^{(4)e6}$  appears to be precisely (minus) the value of  $\mathcal{I}^{(3)d}$  shown in (4.7). Perhaps this can be traced to the diagrammatic relation that is evident in Fig. 8:  $\mathcal{I}^{(3)d}$  appears in the ‘upper diagonal’ of  $\mathcal{I}^{(4)e6}$ .

## 5. Summary

We have classified all four-point dual conformal Feynman diagrams through four loops. In addition to the previously known  $(1, 1, 2, 8)$  integrals (Fig. 6) that contribute to the dimensionally-regulated on-shell amplitude respectively at  $(1, 2, 3, 4)$  loops, we find  $(0, 0, 2, 9)$  new dual conformal integrals (Fig. 8) that vanish on-shell in  $D = 4 - 2\epsilon$  but not off-shell in  $D = 4$ . There are also  $(0, 0, 0, 11)$  dual conformal diagrams (Figs. 7 and 9) that diverge in four dimensions even when taken off-shell and therefore do not give rise to true dual conformal integrals.

Next we addressed the problem of evaluating new off-shell integrals in four dimensions. Of the total number  $(1, 1, 4, 17)$  of such integrals, explicit results for  $(1, 1, 2, 5)$  have appeared previously in [4,23]. We find Mellin-Barnes representations for an additional  $(0, 0, 2, 8)$  integrals, including two pairs related by new ‘magic identities’, and evaluate their infrared singularity structure explicitly. Evaluation of the remaining  $(0, 0, 0, 4)$  integrals  $\mathcal{I}^{(4)f}$ ,  $\mathcal{I}^{(4)f'}$ ,  $\mathcal{I}^{(4)e2'}$ , and  $\mathcal{I}^{(4)c'}$  is left for future work.

## Acknowledgments

We have benefited from discussions with A. Jevicki, Z. Bern, D. Kosower and J. Maldacena and are grateful to F. Cachazo for collaboration in the early stages of this work. The research of MS is supported by NSF grant PHY-0610259 and by an OJI award under DOE grant DE-FG02-91ER40688. The research of AV is supported by NSF CAREER Award PHY-0643150 and by DOE grant DE-FG02-91ER40688.

## References

- [1] M. B. Green, J. H. Schwarz and L. Brink, “ $\mathcal{N} = 4$  Yang-Mills And  $\mathcal{N} = 8$  Supergravity As Limits Of String Theories,” Nucl. Phys. B **198**, 474 (1982).
- [2] P. Nogueira, “Automatic Feynman graph generation,” J. Comput. Phys. **105**, 279 (1993).
- [3] N. I. Usyukina and A. I. Davydychev, “An Approach to the evaluation of three and four point ladder diagrams,” Phys. Lett. B **298**, 363 (1993).
- [4] N. I. Usyukina and A. I. Davydychev, “Exact results for three and four point ladder diagrams with an arbitrary number of rungs,” Phys. Lett. B **305**, 136 (1993).
- [5] D. J. Broadhurst, “Summation of an infinite series of ladder diagrams,” Phys. Lett. B **307**, 132 (1993).
- [6] Z. Bern, L. J. Dixon, D. C. Dunbar and D. A. Kosower, “One loop  $n$  point gauge theory amplitudes, unitarity and collinear limits,” Nucl. Phys. B **425**, 217 (1994) [arXiv:hep-ph/9403226].
- [7] Z. Bern, L. J. Dixon, D. C. Dunbar and D. A. Kosower, “Fusing gauge theory tree amplitudes into loop amplitudes,” Nucl. Phys. B **435**, 59 (1995) [arXiv:hep-ph/9409265].
- [8] Z. Bern, J. S. Rozowsky and B. Yan, “Two-loop four-gluon amplitudes in  $\mathcal{N} = 4$  super-Yang-Mills,” Phys. Lett. B **401**, 273 (1997) [arXiv:hep-ph/9702424].
- [9] Z. Bern, L. J. Dixon and D. A. Kosower, “One-loop amplitudes for  $e^+e^-$  to four partons,” Nucl. Phys. B **513**, 3 (1998) [arXiv:hep-ph/9708239].
- [10] V. A. Smirnov, “Analytical result for dimensionally regularized massless on-shell double box,” Phys. Lett. B **460**, 397 (1999) [arXiv:hep-ph/9905323].
- [11] J. B. Tausk, “Non-planar massless two-loop Feynman diagrams with four on-shell legs,” Phys. Lett. B **469**, 225 (1999) [arXiv:hep-ph/9909506].
- [12] K. Kajantie, M. Laine and Y. Schroder, “A simple way to generate high order vacuum graphs,” Phys. Rev. D **65**, 045008 (2002) [arXiv:hep-ph/0109100].
- [13] A. P. Isaev, “Multi-loop Feynman integrals and conformal quantum mechanics,” Nucl. Phys. B **662**, 461 (2003) [arXiv:hep-th/0303056].
- [14] C. Anastasiou, Z. Bern, L. J. Dixon and D. A. Kosower, “Planar amplitudes in maximally supersymmetric Yang-Mills theory,” Phys. Rev. Lett. **91**, 251602 (2003) [arXiv:hep-th/0309040].
- [15] T. Hahn, “CUBA: A library for multidimensional numerical integration,” Comput. Phys. Commun. **168**, 78 (2005) [arXiv:hep-ph/0404043].
- [16] R. Britto, F. Cachazo and B. Feng, “Generalized unitarity and one-loop amplitudes in  $\mathcal{N} = 4$  super-Yang-Mills,” Nucl. Phys. B **725**, 275 (2005) [arXiv:hep-th/0412103].
- [17] Z. Bern, L. J. Dixon and V. A. Smirnov, “Iteration of planar amplitudes in maximally supersymmetric Yang-Mills theory at three loops and beyond,” Phys. Rev. D **72**, 085001 (2005) [arXiv:hep-th/0505205].

- [18] E. I. Buchbinder and F. Cachazo, “Two-loop amplitudes of gluons and octa-cuts in  $\mathcal{N} = 4$  super Yang-Mills,” *JHEP* **0511**, 036 (2005) [arXiv:hep-th/0506126].
- [19] M. Czakon, “Automatized analytic continuation of Mellin-Barnes integrals,” *Comput. Phys. Commun.* **175**, 559 (2006) [arXiv:hep-ph/0511200].
- [20] F. Cachazo, M. Spradlin and A. Volovich, “Hidden beauty in multiloop amplitudes,” *JHEP* **0607**, 007 (2006) [arXiv:hep-th/0601031].
- [21] F. Cachazo, M. Spradlin and A. Volovich, “Iterative structure within the five-particle two-loop amplitude,” *Phys. Rev. D* **74**, 045020 (2006) [arXiv:hep-th/0602228].
- [22] Z. Bern, M. Czakon, D. A. Kosower, R. Roiban and V. A. Smirnov, “Two-loop iteration of five-point  $\mathcal{N} = 4$  super-Yang-Mills amplitudes,” *Phys. Rev. Lett.* **97**, 181601 (2006) [arXiv:hep-th/0604074].
- [23] J. M. Drummond, J. Henn, V. A. Smirnov and E. Sokatchev, “Magic identities for conformal four-point integrals,” *JHEP* **0701**, 064 (2007) [arXiv:hep-th/0607160].
- [24] Z. Bern, M. Czakon, L. J. Dixon, D. A. Kosower and V. A. Smirnov, “The Four-Loop Planar Amplitude and Cusp Anomalous Dimension in Maximally Supersymmetric Yang-Mills Theory,” *Phys. Rev. D* **75**, 085010 (2007) [arXiv:hep-th/0610248].
- [25] F. Cachazo, M. Spradlin and A. Volovich, “Four-Loop Cusp Anomalous Dimension From Obstructions,” *Phys. Rev. D* **75**, 105011 (2007) [arXiv:hep-th/0612309].
- [26] Z. Bern, J. J. M. Carrasco, H. Johansson and D. A. Kosower, “Maximally supersymmetric planar Yang-Mills amplitudes at five loops,” arXiv:0705.1864 [hep-th].
- [27] L. F. Alday and J. Maldacena, “Gluon scattering amplitudes at strong coupling,” *JHEP* **0706**, 064 (2007) [arXiv:0705.0303 [hep-th]].
- [28] E. I. Buchbinder, “Infrared Limit of Gluon Amplitudes at Strong Coupling,” *Phys. Lett. B* **654**, 46 (2007) [arXiv:0706.2015 [hep-th]].
- [29] J. M. Drummond, G. P. Korchemsky and E. Sokatchev, “Conformal properties of four-gluon planar amplitudes and Wilson loops,” arXiv:0707.0243 [hep-th].
- [30] A. Brandhuber, P. Heslop and G. Travaglini, “MHV Amplitudes in  $\mathcal{N} = 4$  Super Yang-Mills and Wilson Loops,” arXiv:0707.1153 [hep-th].
- [31] F. Cachazo, M. Spradlin and A. Volovich, “Four-Loop Collinear Anomalous Dimension in  $\mathcal{N} = 4$  Yang-Mills Theory,” arXiv:0707.1903 [hep-th].
- [32] M. Kruczenski, R. Roiban, A. Tirziu and A. A. Tseytlin, “Strong-coupling expansion of cusp anomaly and gluon amplitudes from quantum open strings in  $AdS_5 \times S^5$ ,” arXiv:0707.4254 [hep-th].
- [33] J. M. Drummond, J. Henn, G. P. Korchemsky and E. Sokatchev, “On planar gluon amplitudes/Wilson loops duality,” arXiv:0709.2368 [hep-th].